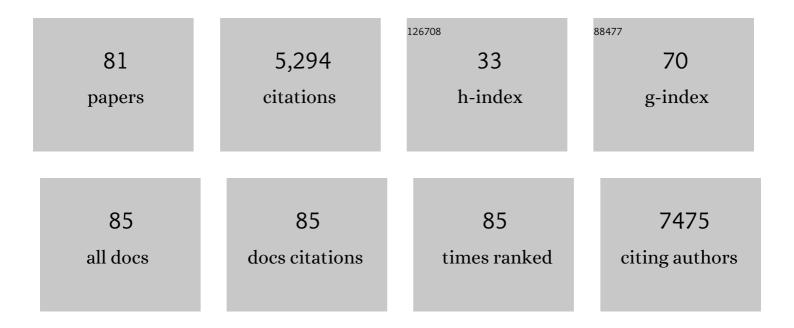
Hans Hebert

List of Publications by Year in descending order

Source: https://exaly.com/author-pdf/3937752/publications.pdf Version: 2024-02-01



#	Article	IF	CITATIONS
1	A Novel N-terminal Region to Chromodomain in CHD7 is Required for the Efficient Remodeling Activity. Journal of Molecular Biology, 2021, 433, 167114.	2.0	4
2	The Polyglutamine Expansion at the N-Terminal of Huntingtin Protein Modulates the Dynamic Configuration and Phosphorylation of the C-Terminal HEAT Domain. Structure, 2020, 28, 1035-1050.e8.	1.6	24
3	Crocus-derived compounds alter the aggregation pathway of Alzheimer's Disease - associated beta amyloid protein. Scientific Reports, 2020, 10, 18150.	1.6	18
4	Recombinant Bri3 BRICHOS domain is a molecular chaperone with effect against amyloid formation and non-fibrillar protein aggregation. Scientific Reports, 2020, 10, 9817.	1.6	16
5	Arachidonic acid promotes the binding of 5-lipoxygenase on nanodiscs containing 5-lipoxygenase activating protein in the absence of calcium-ions. PLoS ONE, 2020, 15, e0228607.	1.1	5
6	Augmentation of Bri2 molecular chaperone activity against amyloid-β reduces neurotoxicity in mouse hippocampus in vitro. Communications Biology, 2020, 3, 32.	2.0	42
7	Cryoâ€EM structure of native human uromodulin, a zona pellucida module polymer. EMBO Journal, 2020, 39, e106807.	3.5	31
8	Aldehyde-alcohol dehydrogenase forms a high-order spirosome architecture critical for its activity. Nature Communications, 2019, 10, 4527.	5.8	39
9	CryoEM: a crystals to single particles round-trip. Current Opinion in Structural Biology, 2019, 58, 59-67.	2.6	4
10	Structural basis of recognition and destabilization of the histone H2B ubiquitinated nucleosome by the DOT1L histone H3 Lys79 methyltransferase. Genes and Development, 2019, 33, 620-625.	2.7	73
11	Granule-stored MUC5B mucins are packed by the non-covalent formation of N-terminal head-to-head tetramers. Journal of Biological Chemistry, 2018, 293, 5746-5754.	1.6	50
12	A spidroinâ€derived solubility tag enables controlled aggregation of a designed amyloid protein. FEBS Journal, 2018, 285, 1873-1885.	2.2	32
13	Integrative Structural Investigation on the Architecture of Human Importin4_Histone H3/H4_Asf1a Complex and Its Histone H3 Tail Binding. Journal of Molecular Biology, 2018, 430, 822-841.	2.0	17
14	Structural modelling of the DNAJB6 oligomeric chaperone shows a peptide-binding cleft lined with conserved S/T-residues at the dimer interface. Scientific Reports, 2018, 8, 5199.	1.6	43
15	Biomimetic spinning of artificial spider silk from a chimeric minispidroin. Nature Chemical Biology, 2017, 13, 262-264.	3.9	231
16	Efficient protein production inspired by how spiders make silk. Nature Communications, 2017, 8, 15504.	5.8	102
17	RNA activationâ€independent DNA targeting of the Type III CRISPR as system by a Csm complex. EMBO Reports, 2017, 18, 826-840.	2.0	23
18	Structural model of dodecameric heat-shock protein Hsp21: Flexible N-terminal arms interact with client proteins while C-terminal tails maintain the dodecamer and chaperone activity. Journal of Biological Chemistry, 2017, 292, 8103-8121.	1.6	24

#	Article	IF	CITATIONS
19	The normal trachea is cleaned by MUC5B mucin bundles from the submucosal glands coated with the MUC5AC mucin. Biochemical and Biophysical Research Communications, 2017, 492, 331-337.	1.0	92
20	Dead-end complex, lipid interactions and catalytic mechanism of microsomal glutathione transferase 1, an electron crystallography and mutagenesis investigation. Scientific Reports, 2017, 7, 7897.	1.6	14
21	Structures of apolipoprotein A-I in high density lipoprotein generated by electron microscopy and biased simulations. Biochimica Et Biophysica Acta - General Subjects, 2017, 1861, 2726-2738.	1.1	2
22	Bri2 BRICHOS client specificity and chaperone activity are governed by assembly state. Nature Communications, 2017, 8, 2081.	5.8	67
23	Method to Visualize and Analyze Membrane Interacting Proteins by Transmission Electron Microscopy. Journal of Visualized Experiments, 2017, , .	0.2	7
24	Structural and Functional Analysis of Calcium Ion Mediated Binding of 5-Lipoxygenase to Nanodiscs. PLoS ONE, 2016, 11, e0152116.	1.1	8
25	Molecular Architecture of Yeast Chromatin Assembly Factor 1. Scientific Reports, 2016, 6, 26702.	1.6	26
26	Shell thickness determination of polymer-shelled microbubbles using transmission electron microscopy. Micron, 2016, 85, 39-43.	1.1	9
27	Huntingtin's spherical solenoid structure enables polyglutamine tract-dependent modulation of its structure and function. ELife, 2016, 5, e11184.	2.8	52
28	A Refined Single-Particle Reconstruction Procedure to Process Two-Dimensional Crystal Images from Transmission Electron Microscopy. Microscopy and Microanalysis, 2015, 21, 876-885.	0.2	5
29	Two-Dimensional Crystallization Procedure, from Protein Expression to Sample Preparation. BioMed Research International, 2015, 2015, 1-10.	0.9	2
30	Investigation of the elimination process of a multimodal polymer-shelled contrast agent in rats using ultrasound and transmission electron microscopy. Biomedical Spectroscopy and Imaging, 2015, 4, 81-93.	1.2	7
31	Free RCK Arrangement in Kch, a Putative Escherichia coli Potassium Channel, as Suggested by Electron Crystallography. Structure, 2015, 23, 199-205.	1.6	3
32	Peptide Anchor for Folate-Targeted Liposomal Delivery. Biomacromolecules, 2015, 16, 2904-2910.	2.6	34
33	Size controlled protein nanoemulsions for active targeting of folate receptor positive cells. Colloids and Surfaces B: Biointerfaces, 2015, 135, 90-98.	2.5	26
34	Structure of potassium channels. Cellular and Molecular Life Sciences, 2015, 72, 3677-3693.	2.4	187
35	The gut microbiota influences blood-brain barrier permeability in mice. Science Translational Medicine, 2014, 6, 263ra158.	5.8	1,589
36	The projection structure of Kch, a putative potassium channel in Escherichia coli, by electron crystallography. Biochimica Et Biophysica Acta - Biomembranes, 2014, 1838, 237-243.	1.4	6

#	Article	IF	CITATIONS
37	On the interplay of shell structure with low- and high-frequency mechanics of multifunctional magnetic microbubbles. Soft Matter, 2014, 10, 214-226.	1.2	44
38	Intestinal MUC2 Mucin Supramolecular Topology by Packing and Release Resting on D3 Domain Assembly. Journal of Molecular Biology, 2014, 426, 2567-2579.	2.0	36
39	Liposome and protein based stealth nanoparticles. Faraday Discussions, 2013, 166, 417.	1.6	26
40	Calcium and pH-dependent packing and release of the gel-forming MUC2 mucin. Proceedings of the National Academy of Sciences of the United States of America, 2012, 109, 5645-5650.	3.3	265
41	Magnetite Nanoparticles Can Be Coupled to Microbubbles to Support Multimodal Imaging. Biomacromolecules, 2012, 13, 1390-1399.	2.6	73
42	Bicarbonate and functional CFTR channel are required for proper mucin secretion and link cystic fibrosis with its mucus phenotype. Journal of Experimental Medicine, 2012, 209, 1263-1272.	4.2	292
43	Structural properties of functional HDL and variants of apoAâ \in I. FASEB Journal, 2012, 26, 997.5.	0.2	0
44	Subunit arrangement in the dodecameric chloroplast small heat shock protein Hsp21. Protein Science, 2011, 20, 291-301.	3.1	29
45	ATP-Induced Conformational Dynamics in the AAA+ Motor Unit of Magnesium Chelatase. Structure, 2010, 18, 354-365.	1.6	70
46	Single-particle cryoelectron microscopy analysis reveals the HIV-1 spike as a tripod structure. Proceedings of the National Academy of Sciences of the United States of America, 2010, 107, 18844-18849.	3.3	55
47	Identification of Key Residues Determining Species Differences in Inhibitor Binding of Microsomal Prostaglandin E Synthase-1*. Journal of Biological Chemistry, 2010, 285, 29254-29261.	1.6	68
48	Cryo-EM Reveals Promoter DNA Binding and Conformational Flexibility of the General Transcription Factor TFIID. Structure, 2009, 17, 1442-1452.	1.6	31
49	Two-Dimensional Crystallization of Biological Macromolecules. , 2009, , 95-111.		0
50	Assembly of Kch, a putative potassium channel from Escherichia coli. Journal of Structural Biology, 2009, 168, 288-293.	1.3	4
51	Microsomal glutathione transferase 1 exhibits one-third-of-the-sites-reactivity towards glutathione. Archives of Biochemistry and Biophysics, 2009, 487, 42-48.	1.4	31
52	Exploring the activity of tobacco etch virus protease in detergent solutions. Analytical Biochemistry, 2008, 382, 69-71.	1.1	25
53	Turning of the receptor-binding domains opens up the murine leukaemia virus Env for membrane fusion. EMBO Journal, 2008, 27, 2799-2808.	3.5	15
54	A New Cryo-EM Single-Particle Ab Initio Reconstruction Method Visualizes Secondary Structure Elements in an ATP-Fueled AAA+ Motor. Journal of Molecular Biology, 2008, 375, 934-947.	2.0	44

#	Article	IF	CITATIONS
55	Structural basis for induced formation of the inflammatory mediator prostaglandin E ₂ . Proceedings of the National Academy of Sciences of the United States of America, 2008, 105, 11110-11115.	3.3	139
56	Location of Substrate Binding Sites within the Integral Membrane Protein Microsomal Glutathione Transferase-1â€. Biochemistry, 2007, 46, 2812-2822.	1.2	33
57	The structure of membrane associated proteins in eicosanoid and glutathione metabolism as determined by electron crystallography. Current Opinion in Structural Biology, 2007, 17, 396-404.	2.6	25
58	Structural Basis for Detoxification and Oxidative Stress Protection in Membranes. Journal of Molecular Biology, 2006, 360, 934-945.	2.0	129
59	Transmembrane topology of FRO2, a ferric chelate reductase from Arabidopsis thaliana. Plant Molecular Biology, 2006, 62, 215-221.	2.0	42
60	The cyclin-dependent kinase 8 module sterically blocks Mediator interactions with RNA polymerase II. Proceedings of the National Academy of Sciences of the United States of America, 2006, 103, 15788-15793.	3.3	186
61	Twoâ€Dimensional Crystallization and Electron Crystallography of MAPEG Proteins. Methods in Enzymology, 2005, 401, 161-168.	0.4	3
62	Renal Na,Kâ€ATPase Structure from Cryoâ€electron Microscopy of Twoâ€Dimensional Crystals. Annals of the New York Academy of Sciences, 2003, 986, 9-16.	1.8	10
63	Human Microsomal Prostaglandin E Synthase-1. Journal of Biological Chemistry, 2003, 278, 22199-22209.	1.6	153
64	Projection structure at 8 A resolution of the melibiose permease, an Na-sugar co-transporter from Escherichia coli. EMBO Journal, 2002, 21, 3569-3574.	3.5	44
65	Three-dimensional structure of renal Na,K-ATPase from cryo-electron microscopy of two-dimensional crystals 1 1Edited by M. F. Moody. Journal of Molecular Biology, 2001, 314, 479-494.	2.0	76
66	Evaluation of scanners and CCD cameras for high-resolution TEM of protein crystals and single particles. , 2000, 49, 292-300.		7
67	Electron Crystallography of a Small Membrane-Bound Enzyme, Microsomal Clutathione Transferase. Microscopy and Microanalysis, 2000, 6, 232-233.	0.2	0
68	The projection structure of the membrane protein microsomal glutathione transferase at 3 Ã resolution as determined from two-dimensional hexagonal crystals. Journal of Molecular Biology, 1999, 288, 243-253.	2.0	34
69	The 3.0 Ã projection structure of microsomal glutathione transferase as determined by electron crystallography of p 21212 two-dimensional crystals. Journal of Molecular Biology, 1997, 271, 751-758.	2.0	40
70	The projection structure of Perfringolysin O (Clostridium perfringensÎ, toxin). FEBS Letters, 1993, 319, 125-127.	1.3	81
71	Cryo-electron microscope analysis of frozen-hydrated crystals of Na, K-ATPase Acta Histochemica Et Cytochemica, 1992, 25, 279-285.	0.8	8
72	Two-dimensional crystals of membrane-bound gastric H,K-ATPase. FEBS Letters, 1992, 299, 159-162.	1.3	55

#	Article	IF	CITATIONS
73	Crystalline layers and three-dimensional structure ofStaphylococcus aureus α-toxin. Journal of Molecular Biology, 1990, 214, 299-306.	2.0	43
74	Coexistence of different forms ofNa,K-ATPase in two-dimensional membrane crystals. FEBS Letters, 1990, 268, 83-87.	1.3	11
75	Structure analysis of fibrinogen by electron microscopy and image processing. Journal of Structural Biology, 1988, 98, 312-319.	0.9	13
76	Digitization of electron micrographs: A comparison of three different types of scanners. Journal of Electron Microscopy Technique, 1988, 8, 381-388.	1.1	4
77	Three-dimensional structure of renal Na,K-ATPase determined from two-dimensional membrane crystals of the p1 form. Journal of Structural Biology, 1988, 100, 86-93.	0.9	20
78	Assembly of two-dimensional membrane crystals of Na,K-ATPase. Journal of Structural Biology, 1988, 99, 234-243.	0.9	8
79			